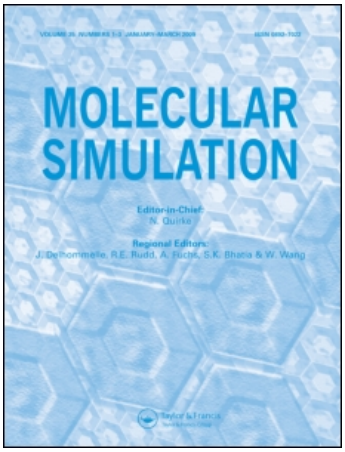

Molecular Simulation
Publication details, including instructions for authors and subscription information:
http://www.informaworld.com/smpp/title~content=t713644482

Further quasi-classical trajectory studies on the $C^+ + H_2O$ reaction

J. R. Flores[a]
[a] Departamento de Química Física, Facultad de Química, Universidad de Vigo, Vigo, Spain

To cite this Article Flores, J. R.(2009) 'Further quasi-classical trajectory studies on the $C^+ + H_2O$ reaction', Molecular Simulation, 35: 4, 325 — 333
To link to this Article: DOI: 10.1080/08927020802430760
URL: http://dx.doi.org/10.1080/08927020802430760

Molecular Simulation
Vol. 35, No. 4, April 2009, 325–333

Taylor & Francis
Taylor & Francis Group

Further quasi-classical trajectory studies on the $C^+ + H_2O$ reaction

J.R. Flores*

Departamento de Química Física, Facultad de Química, Universidad de Vigo, Vigo, Spain

(*Received 30 June 2008; final version received 25 August 2008*)

Further trajectory studies on the $C^+ + H_2O$ reaction have been performed using a potential energy surface described through a finite element method in its *p* version. In former trajectory studies [Y. Ishikawa, T. Ikegami and R.C. Binning Jr., *Direct* ab initio *molecular dynamics study of* $C^+ + H_2O$*: angular distribution of products and distribution of product kinetic energies*, Chem. Phys. Lett. 370 (2003), pp. 490–495; J.R. Flores, *Quasichemical trajectories on a finite element density functional potential energy surface: the* $C^+ + H_2O$ *reaction revisited*, J. Chem. Phys. 125 (2006), 164309], tunnelling was not taken into account. The present results together with the analysis of the electronic excited states [J.R. Flores and A.B. González, *The role of the excited electronic states in the* $C^+ + H_2O$ *reaction*, J. Chem. Phys. 128 (2008), 144310] are useful to interpret the mechanism of the title reaction, which has been the subject of crossed beam experiments [D.M. Sonnenfroh, R.A. Curtiss and J.M. Farrar, *Collision complex formation in the reaction of* C^+ *with* H_2O, J. Chem. Phys. 83 (1985), pp. 3958–3964] and can be considered a prototypical ion–molecule reaction.

Keywords: quasi-classical trajectories; FEM; ion–molecule reactions; tunnelling; molecular astrophysics

1. Introduction

The formyl and isoformyl cations are molecular species of great astrophysical importance [1–6]. One of the reactions that can generate the $[HCO]^+$ system in the space is

$$C^+ + H_2O \rightarrow [HCO]^+ + H.$$

It has been studied experimentally by Rowe et al. [7] for thermal conditions at $T = 300\,K$ and by Marquette et al. [8] at low temperatures in the range of 27–163 K. They have used the CRESU technique (reaction kinetics in uniform supersonic flow). There is a very detailed experimental study using the crossed beam technique by Sonnenfroh et al. [9] (see also [10]). This study has been performed at two particular collision energies, namely 0.62 and 2.14 eV. The authors have concluded that there are two reaction mechanisms: a direct one in which hydrogen is expelled as soon as the collision complex is formed (a 'knockout' mechanism) and a slow one in which the collision complex becomes a relatively long-lived intermediate. Although they have not been able to determine branching ratios, they have concluded that HCO^+ should be at least 30% of the products. They hypothesised, based partly on the *ab initio* computations available at the time [11], that $HCOH^+$ would be the long-lived reaction intermediate, which could evolve towards both the formyl and the isoformyl cations [9,10].

The method of quasi-classical trajectories has been applied quite recently to the study of the title reaction. Ishikawa et al. [12,13] have performed a direct dynamics study at the QCISD/6-31+G* level. Contrary to the crossed beam experiments, they have found virtually no flux towards HCO^+ (at 0.62 eV). They have also concluded that COH_2^+ rather than $HCOH^+$ is the main intermediate. The present author has performed another study using an analytical potential energy surface (PES) constructed by using a *p* version finite element method (FEM); the PES points have been determined using a geometry-dependent density functional method, which has been calibrated using benchmark *ab initio* computations of the stationary points of the PES [14]. This procedure gives an accurate description of the area of the PES, which should be of critical importance in the reaction dynamics, in particular, to determine the branching ratio. However, the results agree with those of Ishikawa in the point that HCO^+ is almost not formed. There could be two obvious explanations, tunnelling and the contribution of electronic excited states to the dynamics. The excited electronic states of the present system have been examined in a recent paper [15]; the present work is a first attempt to establish whether tunnelling could be a significant effect.

2. Theoretical aspects

2.1 The models

In a previous paper [14], we have introduced a *p* version FEM to describe PES, which has been applied to the PES of ground state $(CH_2O)^+$. The electronic structure method

*Email: flores@uvigo.es

ISSN 0892-7022 print/ISSN 1029-0435 online

DOI: 10.1080/08927020802430760
http://www.informaworld.com

is a DFT/6-31G** approach derived from the B3LYP method [16] in which the parameters are dependent on the geometry. The FEM potential V^{FEM} is combined with a long-range potential $V_{\mathrm{l\text{-}r}}$, which describes the interaction between C^+ and water quite accurately, in such a way that the complete potential is

$$V = V^{\mathrm{FEM}} w + (1 - w) V_{\mathrm{l-r}}, \tag{1}$$

where w is a switching function.

The FEM part has the following general expression:

$$V_m^{\mathrm{FE}}(r_1, r_2, \ldots, r_f) = \sum_{i_1=0}^{L_{m,1}} \sum_{i_2=0}^{L_{m,2}} \cdots \sum_{i_f=0}^{L_{m,f}} C_{\{i\}}^m \prod_{k=1}^{f} X_{i_k}(t_{k,m}), \tag{2}$$

where $\{r_i\}$ are the geometrical coordinates, $C_{\{i\}}^m$ are coefficients and $\{X_{i_k}\}$ are one-dimensional local functions corresponding to the kth geometrical variable. $L_{m,k}$ represents the polynomial order at element m for the r_k coordinate and $t_{k,m}$ is the corresponding intrinsic variable, which can be expressed in terms of the segment's mid-point and half-length $\delta_{k,m}$ (both scalar quantities), in the following way $t_{k,m} = (r_k - \bar{r}_{k,m})/\delta_{k,m}$, with $-1 \leq t_{k,m} \leq 1$. The one-dimensional local functions X_{i_k} are either interpolation $\{I_{0_k}, I_{1_k}\}$ or shape functions $\{S_{1_k}, \ldots, S_{L_{m_k}-1}\}$, where X_{2_k} corresponds to S_{1_k}, which is a second-order polynomial. Only the first type of functions is Lagrangian. The Lagrangian functions have the following expressions in terms of the intrinsic variable: $I_0(t) = (1 - t)/2$ and $I_1(t) = (1 + t)/2$. The shape functions are written generally in terms of the Legendre polynomials $S_j(t) = (P_{j+1}(t) - P_{j-1}(t))/\sqrt{4j+1}$. Note that the interpolation and shape functions are used in a hierarchical way, i.e. if $S_j(t)$ is present in the one-dimensional set corresponding to a coordinate at a particular element, all lower order basis functions, $\{S_{j-1}(t) \ldots, I_0(t), I_1(t)\}$, must be present as well. One can use different basis sets for different coordinates or different segments of each coordinate, which implies that different elements may have different descriptions.

The long-range potential has a relatively complex expression inspired in the work of Vande Linde and Hase [17].

The probability of tunnelling for the case of unimolecular decay (metastable state) is given by [18,19]

$$P_n = \mathrm{e}^{-2A/\hbar}, \tag{3}$$

where P_n is the probability of tunnelling when the system hits the barrier at time t_n (i.e. a turning point is reached) and A is the action integral that can be computed as

$$A = \mathrm{Im} \int_{s_1}^{s_2} p(s) \mathrm{d}s. \tag{4}$$

The probability that the system has not tunnelled, in other words, has survived, at a time t when the trajectory has reached a turning point $k(t)$ times is [20]

$$P_s(t) = \prod_{j=1}^{k(t)} (1 - P_j), \tag{5}$$

so the tunnelling probability is defined as

$$P_t(t) \equiv 1 - P_s(t) \tag{6}$$

and can be computed through the following expression

$$P_t(t) = \sum_{j=1}^{k(t)} P_j (1 - P_{j-1})(1 - P_{j-2}) \cdots (1 - P_1), \tag{7}$$

which, if $P_j \ll 1$ is approximately $\sum_{k=1}^{k(t)} P_k$.

If the probabilities are averaged over initial conditions, we have

$$\langle P_s(t) \rangle = 1 - \langle P_t(t) \rangle. \tag{8}$$

The computation of the average can be performed by using the ensemble of trajectories as shown by Waite and Miller [20].

Of course, the present case is polyatomic so a very important aspect is the way the tunnelling path is defined. The basic principle has been to minimise the action by selecting an appropriate direction in the PES. Taking into account former work [18,21–24], three basic directions have been considered: (1) the direction representative of the process, which, if there is a saddle point, is the normal mode of imaginary frequency, (2) the direction of the vector that connects the current position on the PES with the region of the local minimum corresponding to the product, and (3) the direction of the vector that connects the current position with that of the saddle point.

In case there is no saddle point, one has to choose a coordinate representative of the minimum energy path. In case the product does not have a well-defined local minimum, one has to choose a representative geometry for the product. It happens for instance in bond cleavage processes leading to very loosely bound or non-bound products; in such a case, one could chose a point on the least energy reaction path, where the energy variation is very small and the internal atomic rearrangement within the two moieties has ceased.

In the present case, we have scanned in a range of directions using the following vectors:

$$\begin{aligned} \bar{n}_1 &= N_1 \sum_i^F (r_{\mathrm{TS}}(i) - r_g(i)) \bar{u}_i \\ \bar{n}_2 &= N_2 \sum_i^F (r_{\min}(i) - r_{\mathrm{g}}(i)) n_{\mathrm{TS}}(i)^2 \bar{u}_i, \end{aligned} \tag{9}$$

where $\bar{u}_i$ is the unit vector of the direction of the ith internal coordinate and $r_{TS}(i)$, $r_g(i)$ and $r_{min}(i)$ are the corresponding components of the vector pointing at the transition state ($r_{TS}(i)$), of the vector representing the current geometry ($r_g(i)$) and of the minimum representing the *products*. On the other hand, $n_{TS}(i)$ represents the ith coordinate of the transition vector and $\{N_1,N_2\}$ are normalisation constants. The direction is given by

$$\bar{n}_{12} = N_{12}(\gamma\bar{n}_1 + (1-\gamma)\bar{n}_2), \tag{10}$$

where γ is a variable that is optimised by minimising the action integral. The *sudden* approximation is applied at this step [19,23,25], so the action integral is computed as

$$A = \int_{s_1}^{s_2} [2\mu(V(s) - V(s_1))]^{1/2} \mathrm{d}s, \tag{11}$$

where μ is an effective reduced mass of the tunnelling path and s is the corresponding length.

Given that we consider a tunnelling path corresponding to each of five isomerisation or dissociation processes, we determine five different $\bar{n}_{12}$ vectors, so we will write from now on $\bar{n}_{12}^{(l)}$, $l = 1-5$. Note that the tunnelling vectors determined in this way are dependent only on the molecular geometry and the topology of the PES.

At every time step of a trajectory, we determine whether a turning point on the corresponding direction has been reached. In practice, the computation of the tunnelling vectors corresponding to some processes and the corresponding test for the turning point may be excluded if the molecular geometry makes those particular tunnelling events extremely unlikely, i.e. if the corresponding point on the PES is too far from that of the corresponding saddle point or product.

In case a turning point is reached, a computation of the tunnelling probability is performed. As we have already pointed out, we try to provide an upper bound to the tunnelling probabilities, and we intend to do so by seeking a reduction in the action integral through the introduction of some curvature in the tunnelling path, i.e. by approaching the least action path. That integral is still computed as in Equation (11) where, for simplicity, we have used as the reduced mass that corresponding to the normal mode of imaginary frequency of the saddle point of the process.

We must emphasise that the procedure is designed to help elucidate the reaction mechanism rather than to obtain accurate rates for individual processes. It can be described as follows. First, we have split the tunnelling length into two parts, the separation point being that where the distance to the transition state is minimal. We have that the tunnelling coordinate of process l is given, in principle, by

$$\bar{r}^{(l)}(\xi) = \bar{r}_g + \xi\bar{n}_{12}^{(l)}; \quad 0 \le \xi \le \xi_f^{(l)}. \tag{12}$$

The point closest to the transition state $\bar{r}_{TS}^{(l)}$ is given by $\xi_{TS}^{(l)}$, i.e. $|\bar{r}_{TS}^{(l)} - \bar{r}^{(l)}(\xi_{TS}^{(l)})| \to \min$. A perpendicular contribution to the tunnelling coordinate is defined as follows:

$$\begin{aligned}
&\bar{r}_\perp^{(l)}(\xi) = \bar{s}_\perp^{(l)}(\xi) w^{(l)}(\xi);\\
&w^{(l)}(\xi) = \left(\xi/\xi_{TS}^{(l)}\right)^{1/2} \textit{for } \xi \le \xi_{TS}^{(l)}\\
&w^{(l)}(\xi) = \left((\xi_f - \xi)/(\xi_f - \xi_{TS}^{(l)})\right)^{1/2} \textit{for } \xi_{TS}^{(l)} < \xi \le \xi_f^{(l)},
\end{aligned} \tag{13}$$

where $\bar{s}_\perp^{(l)}(\xi)$ is chosen to be perpendicular to $\bar{n}_{12}^{(l)}$. In practice, the action integral is computed by numerical integration, so ξ takes a number of values $\{\xi_n\}$; we have taken equal-width steps. Then the tunnelling path becomes

$$\bar{r}^{(l)}(\xi) = \bar{r}_g + \xi\bar{n}_{12}^{(l)} + \bar{r}_\perp^{(l)}(\xi). \tag{14}$$

Let us note as $\{\bar{u}_i^{(12)}\}$ a set of $F-1$ orthonormal vectors perpendicular to $\bar{n}_{12}^{(l)}$. We have that $\bar{s}_\perp^{(l)}(\xi_n)$ can be expressed as follows:

$$\bar{s}_\perp^{(l)}(\xi_n) = \sum_j^{F-1} \alpha_j^{(n)} \bar{u}_j^{(12)}. \tag{15}$$

The set of parameters $\{\alpha_j^{(n)}\}$ is derived from the preceding set $\{\alpha_j^{(n-1)}\}$ through the following expression:

$$\alpha_j^{(n)} = \alpha_j^{(n-1)} - \Delta_n(\xi_n - \xi n - 1)^2 \frac{(\partial V/\partial\alpha_j)_n}{2(V(\bar{r}^{(l)}(\xi_n,0)) - V(\bar{r}_g))}, \tag{16}$$

which, if $\Delta_n = 1$, approximately minimises to first-order $(V_n - V(\bar{r}_g))^{1/2}|\bar{r}_n - \bar{r}_{n-1}|$, where $\bar{r}_n = \bar{r}_g + \xi_n\bar{n}_{12}^{(l)} + \bar{s}_\perp^{(l)}(\xi_n)$ and

$$V_n = V\left(\bar{r}_g + \xi_n\bar{n}_{12}^{(l)}\right) + \sum_j^{F-1} (\partial V/\partial\alpha_j)_n \alpha_j + \cdots. \tag{17}$$

We have that $V(\bar{r}^{(l)}(\xi_n,0)) = V(\bar{r}_g + \xi_n\bar{n}_{12}^{(l)})$ and that $(\partial V/\partial\alpha_j)_n$ is computed at $\bar{r}_g + \xi_n\bar{n}_{12}^{(l)}$. In practice, we have found it convenient to include Δ_n which is a scaling parameter and choose its value by minimisation of $(V_n - V(\bar{r}_g))^{1/2}|\bar{r}_n - \bar{r}_{n-1}|$. After the set of parameters $\{\alpha_j^{(n)}\}$ has been determined for all steps, we have a set of points along the tunnelling coordinate $\{\bar{r}^{(l)}(\xi_n)\}$ and we determine the action integral numerically.

We have considered that the following reaction processes may be subject to tunnelling:

(1) $COH_2^+ - TS1H \to COH^+ + H$
(2) $COH_2^+ - TS12 \to HCOH^+$
(3) $HCOH^+ - TS2CH \to COH^+ + H$
(4) $HCOH^+ - TS2OH \to HCO^+ + H$
(5) $H{-}COH^+ \to H + HCO^+$

Table 1. Components of $\bar{r}_{TS}^{(l)}$ and $\bar{r}_{min}^{(l)}$ for the five tunnelling processes considered (Å and degrees) and transition vectors $\bar{n}_{TS}^{(l)}$.[a]

	Process (1)	Process (2)	Process (3)	Process (4)	Process (5)
$\bar{r}_{TS}^{(l)}$					
d(CO)	1.2379	1.3145	1.1407	1.1410	1.1410
$d(OH_1)$	1.4879	1.2287	0.9934	2.1806	1.3052
$d(OH_2)$	1.0050	1.0055	2.5702	1.6025	–
$< COH_1$	128.1	67.8	177.7	11.8	57.0
$< COH_2$	125.9	127.9	58.5	128.1	–
$< COH_1H_2$	180.0	148.8	180.0	0.0	–
$\bar{r}_{min}^{(l)}$					
d(CO)	1.2200	1.2236	1.2200	1.1410	1.1410
$d(OH_1)$	1.6000	2.0143	2.5702	2.1800	2.1600
$d(OH_2)$	1.0050	1.0050	1.0050	1.9	–
$< COH_1$	–	26.3	–	–	0.0
$< COH_2$	180.0	118.6	177.7	128.1	–
$< COH_1H_2$	–	180.0	180.0	–	–
$\bar{n}_{TS}^{(l)}$					
d(CO)	−0.3434	0.2974	−0.0528	−0.1108	0.1405
$d(OH_1)$	0.9251	−0.5587	0.6743	0.0680	0.6953
$d(OH_2)$	0.0116	−0.0224	0.0104	0.9514	0.0000
$< COH_1$	0.0768	0.7688	0.6315	−0.2736	−0.7049
$< COH_2$	0.1421	0.0887	0.3790	0.0563	0.0000
$< COH_1H_2$	0.0000	0.0024	0.0000	0.0003	0.0000

[a]Reduced masses for the tunnelling paths of the five processes are (in u): 1.2439, 1.1406, 1.0637, 1.1299 and 1.2009.

It must be noted that TS2CH is a very loose saddle point; the exact PES is likely not to present one, but it appeared at the QCISD/6-311++G(2df,p) level so it was taken as [14]. Process (5) is an isomerisation process taking place when one of the hydrogen atoms is significantly separated from the COH^+ moiety; the initial structure does not need to be $HCOH^+$, it can be COH_2^+ as well. This process could have been characterised by a second-order saddle point, i.e. by a stationary point with two imaginary frequencies, one corresponding to isomerisation and the other corresponding to the fragmentation movement; however, we have not been able to locate it in the FEM PES.

As we have pointed out above, in a previous quasi-classical trajectory study [14], we found that virtually none of the trajectories generated HCO^+ in contrast with the crossed beam experiments [9,10]. A possible explanation could be that efficient tunnelling in process (4) eventually combined with an increased flux to $HCOH^+$ due to a more efficient tunnelling in process (2) than in process (1) may boost the production of HCO^+.

Tunnelling in processes (1), (3) and (4) correspond to the metastable state case [19]. Tunnelling in process (2) would correspond, in principle, to the asymmetric double well case [19] but it turns out that $HCOH^+$ is usually 'formed' with a very energised H—C bond, so we have considered it as a nearly dissociative path and treated it as a metastable state case. Process (5) has been treated as a barrier penetration case [19], i.e. the expression employed for the tunnelling probability is

$$P_n = 1/(1 + e^{2A/\hbar}). \tag{18}$$

The choice of $\bar{r}_{TS}^{(l)}$ and $\bar{r}_{min}^{(l)}$ for the five paths considered is the following (see the numbers in Table 1). For process (2), we have employed the minimum and transition-state geometries of our FEM PES. In the case of processes (1), (3) and (4), the geometry of the minimum is not well defined for the PES is basically flat for increasing $H—(COH)^+$ distance. In these cases, we define $\bar{r}_{min}^{(l)}$ using the geometry of the corresponding transition state as a reference for the O—H or C—H distance (H being the hydrogen atom which is eliminated), and using the equilibrium geometry of isolated COH^+ or HCO^+ (process (4)) as reference for the corresponding moieties; the rest of the parameters are the same as in $\bar{r}_g$. $\bar{r}_{min}^{(5)}$ is composed of the equilibrium geometry of HCO^+ and $\bar{r}_g$; $\bar{r}_{TS}^{(5)}$ is defined by the geometry of the saddle point of the $HCO^+ \leftrightarrow COH^+$ isomerisation and $\bar{r}_g$.

2.2 Averaging

As we have pointed out in the former section, the survival and tunnelling probabilities must be averaged for the ensemble of trajectories. It is also convenient to perform a time average for each trajectory over the period of the movement of the tunnelling direction [20]. Both tasks have

been accomplished according to the expressions given by Waite and Miller [20].

In the present case, trajectories are started at long C^+—OH_2 distances (15 Å), with being in its vibrational ground state with no rotation. The relative translational energy corresponds to 0.62 eV (i.e. one of the two energies used in the crossed beam study [9,10]). We have also chosen zero orbital angular momentum. Note that it is *not* the case that the collision complex (almost always initially COH_2^+ due to dipole alignment) has the same distribution of the energy among the normal modes in all trajectories; in other words, we do not have a common quantum state of COH_2^+ even if we have a particular quantum state of the collision pair. The ensemble average involves all quantum states of the complex, which can be generated from that state of the collision pair and is quite adequate to determine whether tunnelling can be a relevant effect under the conditions of the experiments. It should also be noted that, although the collision complex (COH_2^+) has a relatively large energy (about 101.6 kcal/mol including ZPE), it is not always the case that the energy excess, which tends to reside initially in the C—O bond, accumulates quickly in the movements related with fragmentation to $COH^+ + H$ or isomerisation into $HCOH^+$, as we will see. In other words, in principle, there is a chance that tunnelling may be competitive with the corresponding classical processes and have a sizeable effect.

The period employed for the time average is the time delay of the first hit of the current trajectory with respect to the earliest first hit within the ensemble. In the present case, which is multi-dimensional, and where we do not have a selection of pure quantum states of the intermediates (i.e. the reactants in reactions (1)–(5) above), it is more adequate than other options such as taking the average of the time delay between successive hits. In any case, we have not found the results to be very sensitive to the choice of the time average.

We have compared two quantities, $\langle P_s(t)\rangle = 1 - \langle P_t(t)\rangle$ (defined in expressions (5)–(8)) and what we note as $\langle P_{s,r}(t)\rangle$, i.e. the survival probability due to reaction of the intermediate without tunnelling. The identity of the reacting intermediate depends of course on the tunnelling process; it is COH_2^+ for (1) and (2), $HCOH^+$ for process (3), etc. A 'reaction' event is *any* (classical) process in which the intermediate disappears, not necessarily that of the tunnelling process. $\langle P_{s,r}(t)\rangle$ has been calculated basically as proposed by Waite and Miller [20], by setting to zero the reaction probability when the intermediate has not reacted and to 1 when it has reacted. Whether the intermediate has reacted is established by checking whether the trajectory has left the PES area corresponding to it, according to the PES partitioning employed in Ref. [14], and making sure it does not hit again a turning point of the corresponding tunnelling process. It happens quite often that after having left the PES area of the intermediate, the trajectory comes again to it; only if it does not reach a turning point during this new stay or subsequent stays, the process is considered a reaction event. The ensemble of trajectories employed to compute the average for a particular process is composed by the subset of trajectories that ever reach a turning point corresponding to that process. Perhaps it should be stressed that a particular trajectory may be active in different tunnelling processes at different times.

Perhaps it should also be stressed that $\langle P_{s,r}(t)\rangle$ has been calculated by taking into account actual 'reaction events' whereas $\langle P_s(t)\rangle$ has been determined by using semi-classical tunnelling probabilities. It should also be noted that, although the use of these two survival probabilities is very much in the spirit of the so-called classical-plus-tunnelling method [20–22], it is a somewhat different approach.

3. Results

In order to assess the importance of tunnelling, we have compared the survival probabilities due to tunnelling $\langle P_s(t)\rangle$ and $\langle P_{s,r}(t)\rangle$; actually we have used the logarithms.

We have used a total of 2400 trajectories (see more details in [14]). This number appeared to be sufficient in view of the results obtained with 600 and 1200 trajectories. For example, the tunnelling rates reported below are coincident within 9% with those obtained with 1200 trajectories, except for process (4) where they agree within 23%. It must be noted that the sampling procedure has been performed using the VENUS 96 program [26]. See also [14] for more details.

3.1 Process (1)

The results are shown in Figures 1 and 2. A total of 901 trajectories give the results of those figures. It is readily seen that both figures have the same structure, with two nearly linear segments. The first segment corresponds to the 'direct' trajectories, i.e. C^+—H_2O collisions giving COH_2^+ in such a way that the O—H stretching mode quickly acquires enough energy to dissociate or, in general, to leave the area of the PES corresponding to COH_2^+, as well as to reach turning points corresponding to process (1). After approximately 22 fs COH_2^+ formation by C^+—H_2O collisions has ceased, and this time is almost exactly when the second segment begins. COH_2^+ further decays due to the energy reorganisation that places enough energy in the fragmentation or isomerisation movements. Moreover, some trajectories that have left the area of the PES corresponding to COH_2^+ return to it and contribute later to a further decrease of $\langle P_s(t)\rangle$ and $\langle P_{s,r}(t)\rangle$. The most important conclusion however is that $\langle P_{s,r}(t)\rangle$ decreases far faster than $\langle P_s(t)\rangle$. For instance, a $\mathrm{Ln}(P(t)) - t$ fitting for the first segment gives an effective rate coefficient of

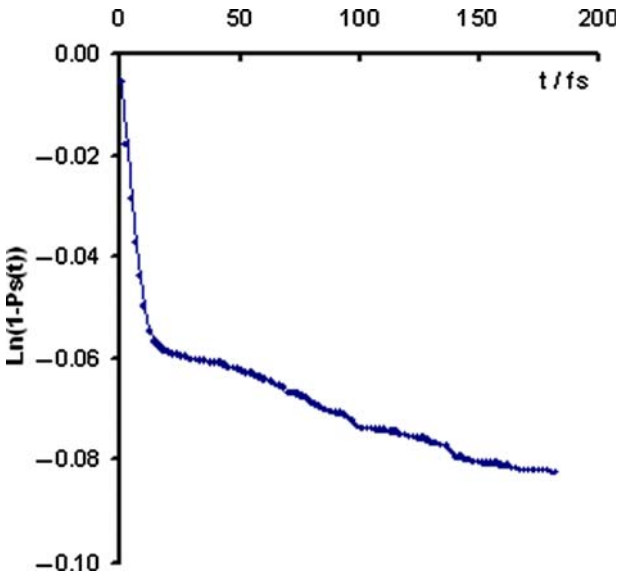

Figure 1. $\mathrm{Ln}(\langle P_s(t)\rangle) - t$ plot for process (1).

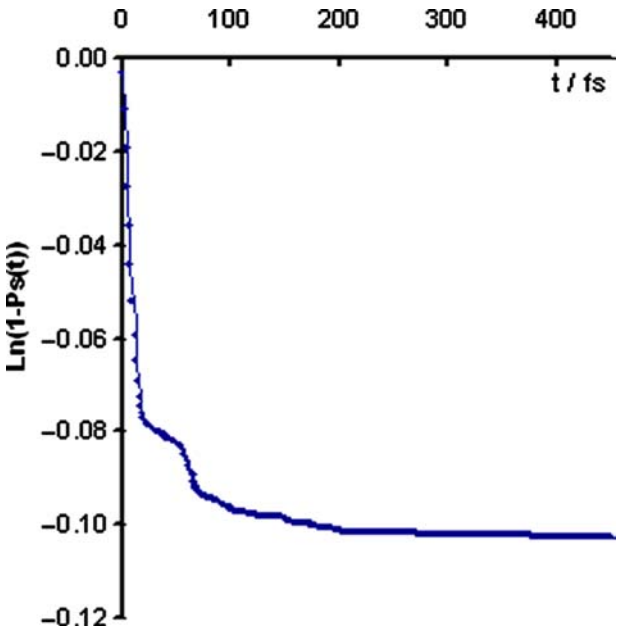

Figure 3. $\mathrm{Ln}(\langle P_s(t)\rangle) - t$ plot for process (2).

$0.094\,\mathrm{fs}^{-1}$ ($\langle P_{s,r}(t)\rangle$) and only $0.006\,\mathrm{fs}^{-1}$ ($\langle P_s(t)\rangle$). This outcome is not difficult to explain; whenever the right normal modes of COH_2^+ are energised enough, there are sizeable probabilities for tunnelling to $COH^+ + H$ but the system is also more likely to leave the PES area corresponding to COH_2^+.

3.2 Process (2)

The results are presented in Figures 3 and 4 and correspond to 959 trajectories. They have basically the same structures as the equivalent figures of process (1) even though that of $\langle P_s(t)\rangle$ is more irregular than that in process (1). Again the first segment corresponds to fast trajectories and shows a similar decay rate as in process (1) ($0.111\,\mathrm{fs}^{-1}$ for $\mathrm{Ln}(\langle P_{s,r}(t)\rangle)$ and $0.006\,\mathrm{fs}^{-1}$ for $\mathrm{Ln}(\langle P_s(t)\rangle)$, which means that, for short times, tunnelling is not a very important effect although it is not insignificant. The time of the transition between the two segments is about 25 fs, i.e. it is very similar to that of process (1). However, the second segment of $\mathrm{Ln}(\langle P_s(t)\rangle)$ is not linear and tends very

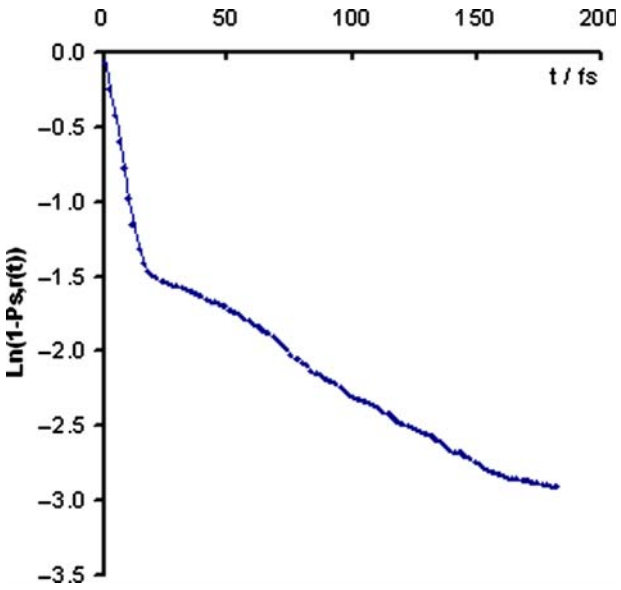

Figure 2. $\mathrm{Ln}(\langle P_{s,r}(t)\rangle) - t$plot for process (1).

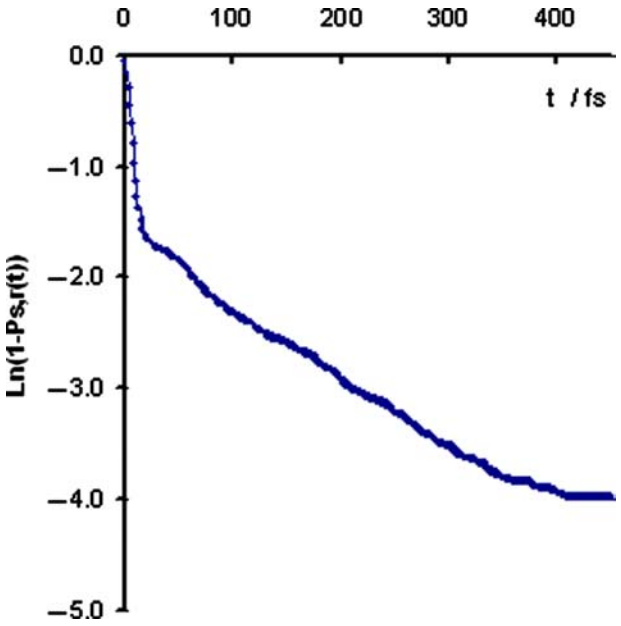

Figure 4. $\mathrm{Ln}(\langle P_{s,r}(t)\rangle) - t$ plot for process (2).

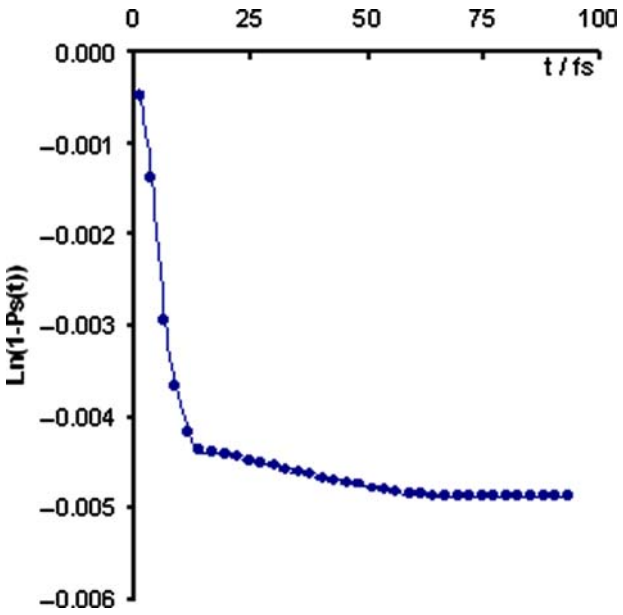

Figure 5. $\mathrm{Ln}(\langle P_s(t)\rangle) - t$ plot for process (4).

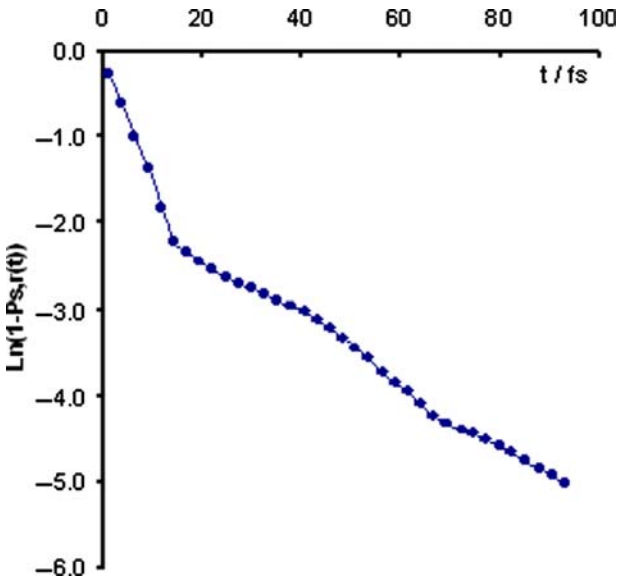

Figure 6. $\mathrm{Ln}(\langle P_{s,r}(t)\rangle) - t$ plot for process (4).

quickly to a nearly constant value; at times longer than 120 fs, the reduction of $\mathrm{Ln}(\langle P_s(t)\rangle)$ is insignificant compared with that of $\mathrm{Ln}(\langle P_{s,r}(t)\rangle)$.

3.3 Process (3)

We have not encountered any meaningful tunnelling flux on process (3). The reason is that TS2CH is a very loose transition state, which may not even exist in the exact PES, so the trajectories can hardly reach a turning point on this path.

3.4 Process (4)

The results are presented in Figures 5 and 6 and correspond to just 31 trajectories. This fact implies that process (4) must be of little relevance for that number implies that only 1.3% of trajectories reach an area of the PES and in conditions such that they may undergo tunnelling through process (4). Even with the limited number of trajectories, it is perceptible that, at short times, the decay rate of $\mathrm{Ln}(\langle P_{s,r}(t)\rangle)$ is rather quick ($0.15\,\mathrm{fs}^{-1}$) whereas that of the tunnelling survival probability is rather slow ($0.0004\,\mathrm{fs}^{-1}$). Moreover, transition to the second segment occurs very early, at about 14 fs, and from that point the effect of tunnelling should be negligible.

3.5 Process (5)

We have encountered that 1871 trajectories are active on process (5), which, as said above, represents mostly a $\mathrm{COH}^+ \leftrightarrow \mathrm{HCO}^+$ isomerisation during fragmentation. The results are shown in Figures 7 and 8. Now even the $\mathrm{Ln}(\langle P_{s,r}(t)\rangle) - t$ plot is quite irregular, at least partly as a consequence of the fact that very ample regions of the PES are involved; for instance, the fragmenting intermediate can be both COH_2^+ and HCOH^+. There is no evidence of efficient tunnelling. The maximum magnitude of the slope of the $\mathrm{Ln}(\langle P_s(t)\rangle) - t$ curve is $-0.0009\,\mathrm{fs}^{-1}$ (in the interval 0–15 fs) when the corresponding value of the $\mathrm{Ln}(\langle P_{s,r}(t)\rangle) - t$ plot is $-0.0399\,\mathrm{fs}^{-1}$ (in the range 0–26 fs). Tunnelling should virtually cease at about 300 fs; the average decay rate due to reaction in the

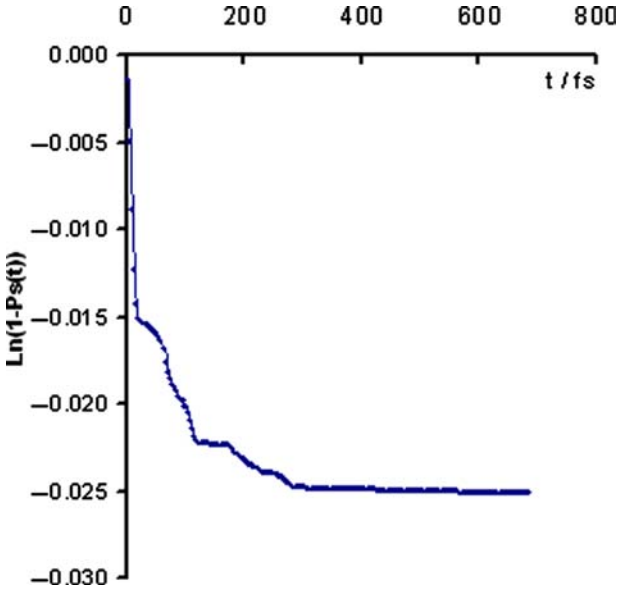

Figure 7. $\mathrm{Ln}(\langle P_s(t)\rangle) - t$ plot for process (5).

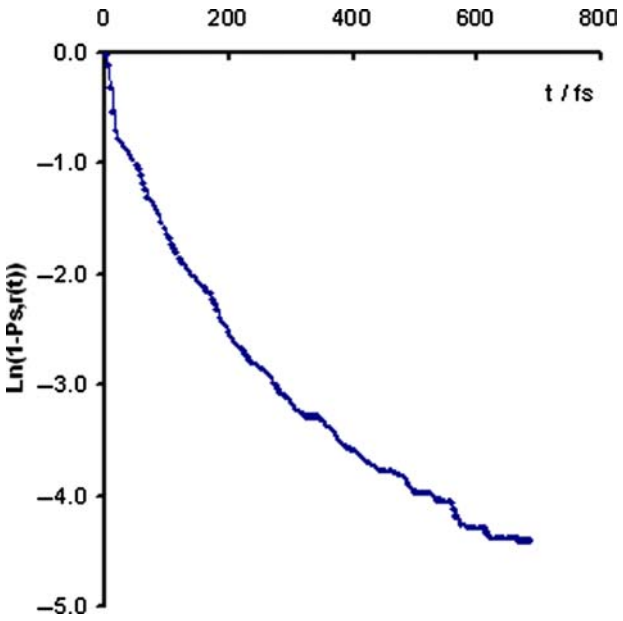

Figure 8. $\mathrm{Ln}(\langle P_{s,r}(t)\rangle) - t$ plot for process (5).

interval 0–300 fs is still 0.0093 fs^{-1}, i.e. 10 times larger than the maximum tunnelling rate.

4. Conclusions

We have performed quasi-classical trajectory computations on the $C^+ + H_2O$ reaction. The potential includes a short-range part, which is described through a FEM method. Former trajectory studies on that reaction differ from a crossed study in the fact that almost no flow towards $HCO^+ + H$ is encountered in the trajectory computations. The present approach includes a procedure to estimate upper bounds of the semi-classical tunnelling probabilities. The incidence of tunnelling has been assessed by comparing the time evolution of the survival probabilities (actually their logarithms) for tunnelling and 'reaction', the latter term meaning basically the disappearance of the intermediate(s) involved in the particular tunnelling process considered. Five possible tunnelling processes have been considered in the evolution of COH_2^+ formed by C^+—H_2O collisions. The sampling procedure for the collision process tries to be coherent with the conditions of the crossed beam experiments of Farrar et al. (in particular, those corresponding to a relative translational energy of 0.62 eV). The results, even if of limited accuracy, due to theoretical and practical limitations, are clear in the following points. First, the process $HCOH^+ \rightarrow HCO^+ + H$ cannot increase significantly its rate by tunnelling. Moreover, the modest increase of the rate of the $COH_2^+ \rightarrow HCOH^+$ isomerisation is quite close to that of the $COH_2^+ \rightarrow COH^+ + H$ fragmentation, so tunnelling should not increase the flux into $HCOH^+$. Finally, a mechanism in which fragmentation towards the products with concurrent isomerisation of the COH^+ moiety into HCO^+, which would explain the generation of the latter isomer, has not been found to present large tunnelling probabilities.

The present results, together with those of a study of the excited electronic states of the COH_2^+ system, suggest that the discrepancies between crossed beam studies and trajectory computations may be due to a significant role of first excited state in the reaction dynamics.

Acknowledgements

The financial support of the Xunta de Galicia through project PGIDT05PXIB315402 PR. The services provided by the 'Centro de Supercomputación de Galicia' (CESGA) are also acknowledged.

References

[1] E. Herbst, N.G. Adams, and D. Smith, *Laboratory measurements of ion-molecular reactions pertaining to interstellar hydrocarbon synthesis*, Astrophys. J. 269 (1983), pp. 329–333.
[2] D. Smith and N.G. Adams, *Molecular synthesis in interstellar clouds: recent laboratory studies of ionic reactions*, Int. Rev. Phys. Chem. 1 (1981), pp. 271–307.
[3] H.-H. Lee, R.P.A. Bettens, and E. Herbst, *Fractional abundances of molecules in dense interstellar clouds: a compendium of recent model results*, Astron. Astrophys. Suppl. Serv. 119 (1996), pp. 111–114.
[4] L.A.M. Nejad and R. Wagenblast, *Time dependent chemical models of spherical dark clouds*, Astron. Astrophys. 350 (1999), pp. 204–229.
[5] C. Savage and L.M. Ziurys, *Ion chemistry in photon-dominated regions, Examining the [HCO^+]/[HOC^+]/[CO^+] chemical network*, Astrophys. J. 616 (2004), pp. 966–975.
[6] H. Liszt, R. Lucas, and J.H. Black, *The abundance of HOC^+ in diffuse clouds*, Astron. Astrophys. 428 (2004), pp. 117–120.
[7] B.R. Rowe, J.B. Marquette, G. Dupeyrat, and E.E. Ferguson, *Reactions of He^+ and N^+ ions with several molecules at 8 K*, Chem. Phys. Lett. 113 (1985), pp. 403–406.
[8] J.B. Marquette, B.R. Rowe, G. Dupeyrat, G. Poissant, and C. Rebrion, *Ion-polar-molecule reactions: a CRESU study of He^+, C^+, N^+ + H_2O, NH_3 at 27, 68 and 163 K*, Chem. Phys. Lett. 122 (1985), pp. 431–435.
[9] M. Sonnenfroh, R.A. Curtiss, and J.M. Farrar, *Collision complex formation in the reaction of C^+ with water*, J. Chem. Phys. 83 (1985), pp. 3958–3964.
[10] J.M. Farrar, in *Advances in Classical Trajectory Methods*, W.L. Hase, ed.,Vol. 2, JAI Press Inc., Greenwich, CT, 1994, pp. 43–93.
[11] Y. Osamura, J.D. Goddard, H.F. Schaefer III, and K.S. Kim, *Near degenerate rearrangement between the radical cations of formaldehyde and hydroxymethylene*, J. Chem. Phys. 74 (1981), pp. 617–624.
[12] Y. Ishikawa, R.C. Binning, Jr., and T. Ikegami, *Direct* ab initio *molecular dynamics study of C^++H_2O*, Chem. Phys. Lett. 343 (2001), pp. 413–419.
[13] Y. Ishikawa, T. Ikegami, and R.C. Binning, Jr., *Direct* ab initio *molecular dynamics study of C^++H_2O: angular distribution of products and distribution of product kinetic energies*, Chem. Phys. Lett. 370 (2003), pp. 490–495.
[14] J.R. Flores, *Quasiclassical trajectories on a finite element density functional potential energy surface: the C^++H_2O reaction revisited*, J. Chem. Phys. 125 (2006), 164309.
[15] J.R. Flores and A.B. González, *The role of the excited electronic states in the C^++H_2O reaction*, J. Chem. Phys. 128 (2008), 144310.

[16] A.D. Becke, *Density-functional thermochemistry. III. The role of exact exchange*, J. Chem. Phys. 98 (1993), pp. 5648–5652.
[17] S.R. Vande Linde and W.L. Hase, *Complete multidimensional analytic potential energy surface for chloride + chloroform SN2 nucleophilic substititution*, J. Phys. Chem. 94 (1990), pp. 2778–2788.
[18] N. Makri and W.H. Miller, *A semiclassical tunneling model for use in classical trajectory simulations*, J. Chem. Phys. 91 (1989), pp. 4026–4036.
[19] Y. Guo and D.L. Thompson, in *Modern Methods for Multidimensional Dynamics Computations in Chemistry*, D. L. Thompson, ed., World Scientific, Singapore, 1998.
[20] B.A. Waite and W.H. Miller, *Model studies of mode specificity in unimolecular reaction dynamics*, J. Chem. Phys. 73 (1980), pp. 3713–3721.
[21] Y. Qin and D.L. Thompson, *Semiclassical treatment of tunneling effects in HONO cis-trans isomerization*, J. Chem. Phys. 100 (1994), pp. 6445–6457.
[22] B.A. Waite, *A classical plus tunneling model for unimolecular reaction dynamics: the hydrogen isocyanide → hydrogen cyanide isomerization*, J. Phys. Chem. 88 (1984), pp. 5076–5083.
[23] J.M. Gómez-LLorente and E. Pollak, *Quasiclassical trajectory method for tunneling rates in the unimolecular decomposition of H_3^+*, Chem. Phys. 120 (1988), pp. 37–49.
[24] T.D. Sewell, Y. Guo, and D.L. Thompson, *Semiclassical calculations of tunneling splitting in malonaldehyde*, J. Chem. Phys. 103 (1995), pp. 8557–8565.
[25] Y. Guo and D.L. Thompson, *A multidimensional semiclassical approach for coupled-coordinate tunneling: level splitting in α-methyl-β-hydroxyacrolein*, J. Chem. Phys. 105 (1996), pp. 1070–1073.
[26] W.L. Hase, R.J. Duchovic, X. Hu, A. Komornicki, K.F. Lim, D. Lu, G.H. Peslherbe, K.N. Swamy, S.R. Vande Linde, A. Varandas, H. Wang, and R. Wolf, *Venus 96, A General Chemical Dynamics Computer Program*, QCPE Bull. 16 (1996), p. 43.